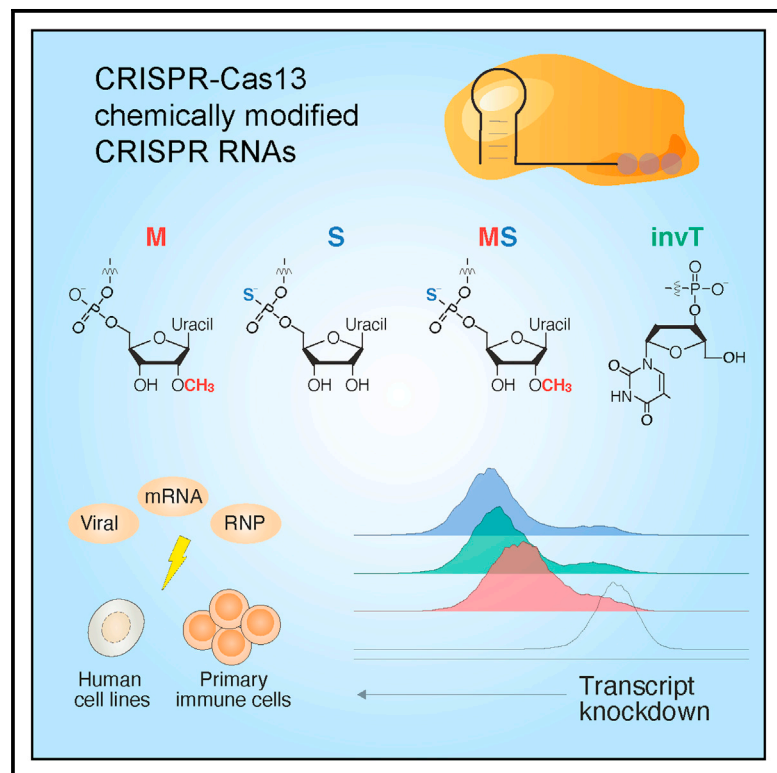


Cell Chemical Biology

Chemically modified guide RNAs enhance CRISPR-Cas13 knockdown in human cells

Graphical abstract



Authors

Alejandro Méndez-Mancilla,
Hans-Hermann Wessels,
Mateusz Legut, ..., G. Brett Robb,
Kevin Holden, Neville E. Sanjana

Correspondence

neville@sanjanalab.org

In brief

By screening multiple chemical modifications of the CRISPR RNA (crRNA), Méndez-Mancilla et al. identify specific chemical modifications and placement of modified bases that improve CRISPR-Cas13 transcript knockdown in human cells. The authors demonstrate that Cas13 ribonucleoproteins complexed with chemically modified crRNAs can modify the transcriptome of human primary T cells.

Highlights

- Chemical modification of Cas13 guide RNAs improves RNA targeting in human cells
- Modifications at the guide RNA 3' end increase Cas13 activity and prolong knockdown
- Cas13 ribonucleoproteins yield high knockdown in human primary immune cells

Brief Communication

Chemically modified guide RNAs enhance CRISPR-Cas13 knockdown in human cells

Alejandro Méndez-Mancilla,^{1,2,5} Hans-Hermann Wessels,^{1,2,5} Mateusz Legut,^{1,2} Anastasia Kadina,³ Megumu Mabuchi,⁴ John Walker,³ G. Brett Robb,⁴ Kevin Holden,³ and Neville E. Sanjana^{1,2,6,*}

¹New York Genome Center, New York, NY, USA

²Department of Biology, New York University, New York, NY, USA

³Synthego Corporation, Redwood City, CA, USA

⁴New England Biolabs, Ipswich, MA, USA

⁵These authors contributed equally

⁶Lead contact

*Correspondence: neville@sanjanalab.org

<https://doi.org/10.1016/j.chembiol.2021.07.011>

SUMMARY

RNA-targeting CRISPR-Cas13 proteins have recently emerged as a powerful platform to modulate gene expression outcomes. However, protein and CRISPR RNA (crRNA) delivery in human cells can be challenging with rapid crRNA degradation yielding transient knockdown. Here we compare several chemical RNA modifications at different positions to identify synthetic crRNAs that improve RNA targeting efficiency and half-life in human cells. We show that co-delivery of modified crRNAs and recombinant Cas13 enzyme in ribonucleo-protein (RNP) complexes can alter gene expression in primary CD4⁺ and CD8⁺ T cells. This system represents a robust and efficient method to modulate transcripts without genetic manipulation.

INTRODUCTION

The CRISPR-Cas13 enzyme family has shown remarkable versatility in basic biology and biotechnology applications (Smargon et al., 2020), including RNA knockdown (Abudayyeh et al., 2017; Cox et al., 2017; Konermann et al., 2018; Smargon et al., 2020), transcript modifications like RNA editing (Cox et al., 2017; Li et al., 2020), live imaging (Wang et al., 2019; Yang et al., 2019), and diagnostics (Gootenberg et al., 2017, 2018; Barnes et al., 2020). Importantly, CRISPR-based transcriptome modulation has been proposed to offer considerable therapeutic potential for a wide spectrum of RNA-mediated diseases (Granados-Riveron and Aquino-Jarquin, 2018; Freije et al., 2019; Smargon et al., 2020). In all cases, a CRISPR RNA (crRNA) guides Cas13 to its target RNA by RNA-RNA hybridization of a short ~23-nt spacer sequence to the target site (Zhang et al., 2018; Wessels et al., 2020). Cas13-based effectors act on the RNA level and do not result in permanent changes to the genome. However, without a continuous source of crRNA expression, effects are short-lived due to rapid crRNA degradation by endogenous RNA nucleases and regeneration of the cellular steady state by continuous target RNA expression.

Although continuous crRNA expression can be achieved via genetic manipulation, such as viral vectors expressing the crRNA and/or Cas13 (Abudayyeh et al., 2017; Konermann et al., 2018; Cui et al., 2020), these methods are less desirable for more physiologically relevant or therapeutic settings, such as targeting of immune checkpoints for immuno-oncology or differentiation of autologous stem cells prior to transplantation (Smith et al.,

2017; Ribas and Wolchok, 2018). One of the main challenges for transcriptome manipulations is to achieve efficient delivery of CRISPR systems for robust RNA manipulation without modifying host DNA sequence. Recently, others have demonstrated chemical activation of crRNAs for Cas13a cleavage *in vitro* (Wang et al., 2020) and delivered recombinant Cas13d into zebrafish embryos (Kushawah et al., 2020). However, it remains unclear if a similar approach in human cells can lead to lasting effects. Inspired by guide RNA modifications for DNA-targeting Cas9 and Cas12a nucleases (Hendel et al., 2015; Lee et al., 2017; Yin et al., 2017; Cromwell et al., 2018; McMahon et al., 2018; Ryan et al., 2018; Jiang et al., 2020), we sought to test if chemically modified synthetic crRNAs can be delivered into human cells to enhance Cas13-mediated transcript knockdown.

RESULTS

Cas13 crRNA chemical modifications improve transcript knockdown

First, we assessed the degree of target RNA knockdown upon exogenous delivery of unmodified and chemically modified crRNAs. We synthesized crRNAs with different chemical modifications at three uridine nucleotides (3xU) at the 3' end of a 23-nt spacer sequence or with an inverted thymidine (invT) capping the 3' end (Figure 1A). We tested three different modifications of the 3xU bases that have been reported before to improve RNA stability and evade secondary immune responses (Hendel et al., 2015; Lee et al., 2017; Wienert et al., 2018): 2'-O-methylation (M), phosphorothioate linkage (S), and 2'-O-methylation and

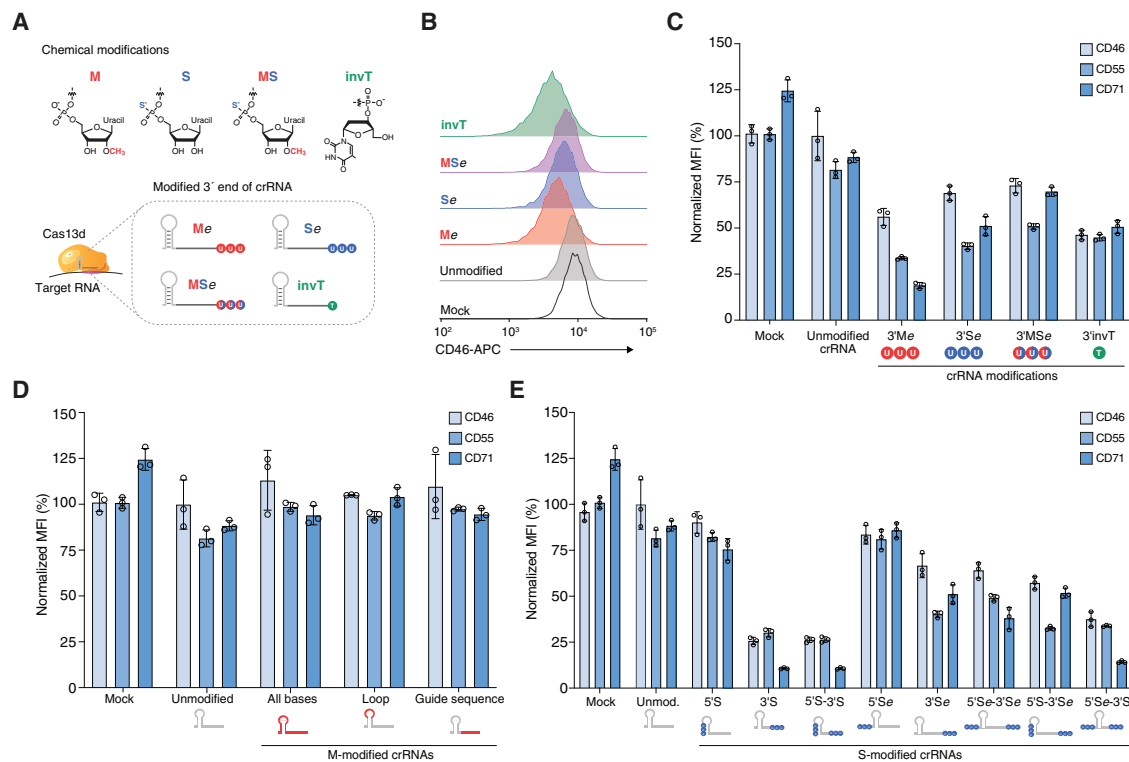


Figure 1. Chemically modified crRNAs improve Cas13 knockdown in human cells

(A) Overview of chemical modifications incorporated during synthesis of crRNAs: M, 3'-O-methyl base; S, phosphorothioate bond; MS, 3'-O-methyl base and phosphorothioate bond; invT, inverted thymidine. All crRNA sequences and modifications are listed in Table S1.

(B) Representative flow cytometry results for CD46 knockdown in HEK293FT-TetO-*RfxCas13d*-NLS cells nucleofected with synthetic crRNAs targeting CD46: specifically, three modified uridines (Me, Se, MSe modifications with e denoting an extended crRNA with extra uridines) or an inverted thymidine directly following the last base of the guide sequence (invT modification).

(C–E) Percentage of CD46, CD55, and CD71 protein expression 72 h post-nucleofection with the indicated crRNAs in HEK293FT-TetO-*RfxCas13d*-NLS cells. Cas13 expression was induced with doxycycline 24 h prior to crRNA nucleofection. Target protein expression was measured by flow cytometry. RNA modification and placement were as follows: (C) synthetic crRNAs with chemical modifications located in the 3' crRNA end; specifically, three modified uridines (M, S, MS modifications) or directly following the last base of the guide sequence (invT modification). (D) Synthetic crRNAs with 3'-O-methyl (M) modification in all nucleotides in the crRNA (direct repeat and guide), in 3 nt in the loop region of the direct repeat, or in the 23-nt guide sequence. (E) Synthetic crRNAs chemically modified with a phosphorothioate bond placed in the crRNA sequence at the 5' and/or 3' end (S), or in three uridines added at the 5' and/or 3' end (Se). Relative protein expression was calculated by comparing the normalized median fluorescent intensity (MFI) with cells nucleofected with non-targeting crRNAs. Bars represent mean values \pm SD, n = 3 biological replicate nucleofections.

phosphorothioate linkage (MS). These modified crRNAs add extra bases at the crRNA 3' end; however, as we previously have shown, nucleotide mismatches to the target site beyond the 23-nt RNA-RNA hybridization interface do not interfere with target knockdown efficiency (Wessels et al., 2020). We chose to assess target knockdown efficiency of three broadly expressed cell surface proteins (CD46, CD55, CD71) that can be efficiently targeted with *RfxCas13d* (Wessels et al., 2020). The synthesized crRNAs were nucleofected into monoclonal *RfxCas13d*-expressing HEK293FT cells and, after 3 days, we quantified protein expression by flow cytometry (Figure S1A). For unmodified crRNAs, we noticed that protein knockdown for each of the three target transcripts was barely detectable relative to non-targeting crRNAs, suggesting that unmodified crRNAs get rapidly cleared in human cells and cannot yield lasting knockdown effects (Figures 1B, 1C, and S1B). On the other hand, all of the chemically modified crRNAs improved target knockdown but did so to varying degrees (one-way ANOVA,

$p < 10^{-4}$). We found that M-modified crRNAs had the overall largest knockdown (80% knockdown of CD71) but that there was greater variability among targeted transcripts. In contrast, we found that the invT modification improved knockdown efficiency in a more consistent manner across the three cell surface markers (55%) (Figure 1C). Surprisingly, the combination of M and S modifications did not result in improved knockdown compared with either individual (M or S) modification (one-way ANOVA, Tukey-corrected $p = 0.14$ [M], $p = 0.89$ [S]).

In addition to improving Cas13-mediated target knockdown, we wondered if chemical modifications can close the gap between low- and high-efficiency guide sequences. Previously we used a high-throughput crRNA screen to identify optimal Cas13 guide sequence design parameters and developed a scoring metric to predict crRNA efficiency (Guo et al., 2020; Wessels et al., 2020). We chose one low-scoring guide sequence per target gene in addition to the high-scoring guide sequence used above (Figure S2A) and found that chemically modified crRNAs

do not generally improve the activity of low-scoring guide sequences (Figure S2B). This suggests that chemical modifications may improve crRNA stability but do not improve guide sequence efficiency. Stability of the crRNA is a key element of efficient Cas13 knockdown: using M-modified crRNAs, we found that substantial knockdown was only possible when Cas13 was already expressed (Figure S2C), similar to previously reports with Cas9 (Hendel et al., 2015). This suggests that Cas13 protein must be available for efficient ribonucleoprotein (RNP) complex formation after crRNAs are introduced into cells. We found similar results when we introduced Cas13 as messenger RNA at different timepoints relative to crRNA nucleofection (Figures S2D and S2E).

Encouraged by these results, we next examined whether alternative placement of modified bases could further improve crRNA stability and transcript knockdown. Specifically, we tested if more extensively M-modified crRNAs could increase crRNA stability without interfering with target knockdown, as previously shown for DNA-targeting Cas9 sgRNAs (Yin et al., 2017; Cromwell et al., 2018; Ryan et al., 2018). We synthesized crRNAs containing an M modification along all the bases in the crRNA (53 modified bases), all bases in the spacer sequence (23 modified bases), or in the direct repeat loop sequence (three modified bases). For all three targeted genes, these more extensive M modifications abrogated Cas13 knockdown compared with unmodified crRNAs, presumably by disrupting the Cas13-crRNA interaction (Figure 1D). With Cas9 guide RNAs, multiple groups have found that moderate modification at the ends of the guide RNA tend to work best (Lee et al., 2017; Jiang et al., 2020), although one group reported an enhanced guide RNA with a majority of bases modified (~70%) for targeting hepatocytes *in vivo* (Yin et al., 2017). In contrast, our results show that a high degree of chemical modification yields less Cas13d knockdown.

Since partial modifications at the 3' end boost knockdown, we decided to systematically test the effect of partial modifications on the crRNA 5' and 3' ends. We tested crRNAs with S modification at the first and last three nucleotides of the crRNA's 5' and 3' ends (5S and 3S, respectively) or using a 3xU 5' or 3' extension (5'Se and 3'Se, respectively). We also tested all combinations of 5' and 3' end modifications. We found marked improvement of target knockdown for crRNAs with phosphorothioate modifications at the 3' end of the spacer sequence (Figure 1E). Interestingly, 3' phosphorothioate modifications improved knockdown efficiency to a greater degree when placed within the spacer sequence (3'S) compared with being placed in 3xU extensions (3'Se) (two-tailed t test, $p = 0.03$). Modifications at the 5' end of the crRNA alone or in conjunction with 3' modifications did not improve target knockdown efficiency (one-way ANOVA, Tukey-corrected $p = 0.99$ for all comparisons with added 5' modifications). These results suggest that exonucleases or degradation processes at the crRNA 3' end are a major hurdle for increased Cas13 activity using synthetic crRNAs (Basila et al., 2017).

Temporal dynamics of transcript knockdown with chemically modified crRNAs and targeting of a SARS-CoV-2 viral RNA reporter construct

Next, we sought to assess the temporal dynamics of Cas13 activity with synthetic crRNAs by comparing knockdown of CD46 over time for 3' invT, 3'S, and unmodified crRNAs relative to non-targeting crRNAs (Figure 2A). All three targeting crRNAs,

including unmodified crRNAs, yielded almost complete CD46 knockdown at 24 h after nucleofection with 89% protein loss for 3'S-modified crRNAs (Figure 2B). While CD46 expression quickly recovered in cells targeted with unmodified crRNAs, 3'S crRNAs led to pronounced knockdown at 48 h after crRNA delivery (Figure 2C). Even 4 days after nucleofection, the modified crRNAs resulted in ~40% knockdown. Both crRNA modifications extend knockdown effects by about 2 days compared with unmodified crRNAs.

Recently, several groups have suggested the possibility of using Cas13 to target severe acute respiratory syndrome coronavirus 2 (SARS-CoV-2), a positive-sense RNA virus responsible for the current global pandemic of novel coronavirus disease 2019 (COVID-19) (Abbott et al., 2020; Ariziti-Sanz et al., 2020; Blanchard et al., 2021). To test if synthetic crRNAs can degrade SARS-CoV-2, we designed a reporter construct that contains the SARS-CoV-2 leader sequence in the 5' UTR of an EGFP reporter gene (Figure 2D). The SARS-CoV-2 leader sequence is a component of all SARS-CoV-2 subgenomic RNAs and thus represents a universal targeting site for all subgenomic viral transcripts (Lai, 1986; Kim et al., 2020). Similar to our experiments with endogenous human transcripts, we found that 3'S-modified crRNAs targeting the SARS-CoV-2 leader sequence can suppress reporter protein expression, despite targeting an untranslated sequence (Figure 2E). These results suggest that Cas13 together with chemically modified crRNAs may represent an efficient and programmable therapeutic approach to target universal SARS-CoV-2 sequences.

Cas13 RNP complexes with chemically modified crRNAs lead to efficient transcript knockdown in human primary T cells

In addition to delivery of chemically modified crRNAs for extended knockdown, another major challenge is delivery of the effector protein into systems that cannot easily be genetically modified to continuously express Cas13. Therefore, we next sought to evaluate if we could preassemble Cas13 RNP complexes with synthetic crRNAs and deliver these RNPs into primary human cells. First, we confirmed that preassembled RNPs with recombinant RfxCas13d with nuclear localization signals (NLSs) on the N and C termini (rCas13d) could efficiently degrade different target RNAs *in vitro* (Figure 3A and S3A–S3C). We found that purified rCas13d with or without an N-terminal MKIEE expression and solubility tag resulted in similar nuclease activity *in vitro*. By nucleofection of RNPs into human HEK293FT cells, we identified optimal buffer and temperature conditions for RNP assembly, achieving ~85% knockdown of CD46 at 24 h post nucleofection (Figures 3B and S3D). At 48 h post nucleofection, we found that complexing in a Tris-based buffer at an elevated temperature (37°C) led to greater knockdown than an alternative buffer and room temperature RNP formation (two-way ANOVA with Tukey-corrected $p < 10^{-4}$ for buffer and $p < 10^{-3}$ for temperature). We further optimized RNP delivery using different protein amounts, while keeping the molar ratio of rCas13d to crRNA (1:2) constant. We found that 10 μ g of rCas13d protein yielded the strongest knockdown and that additional rCas13d does not lead to greater knockdown (two-tailed t test, $p = 0.7$) (Figure 3C). In agreement with our prior results using viral delivery of Cas13d, we find that using

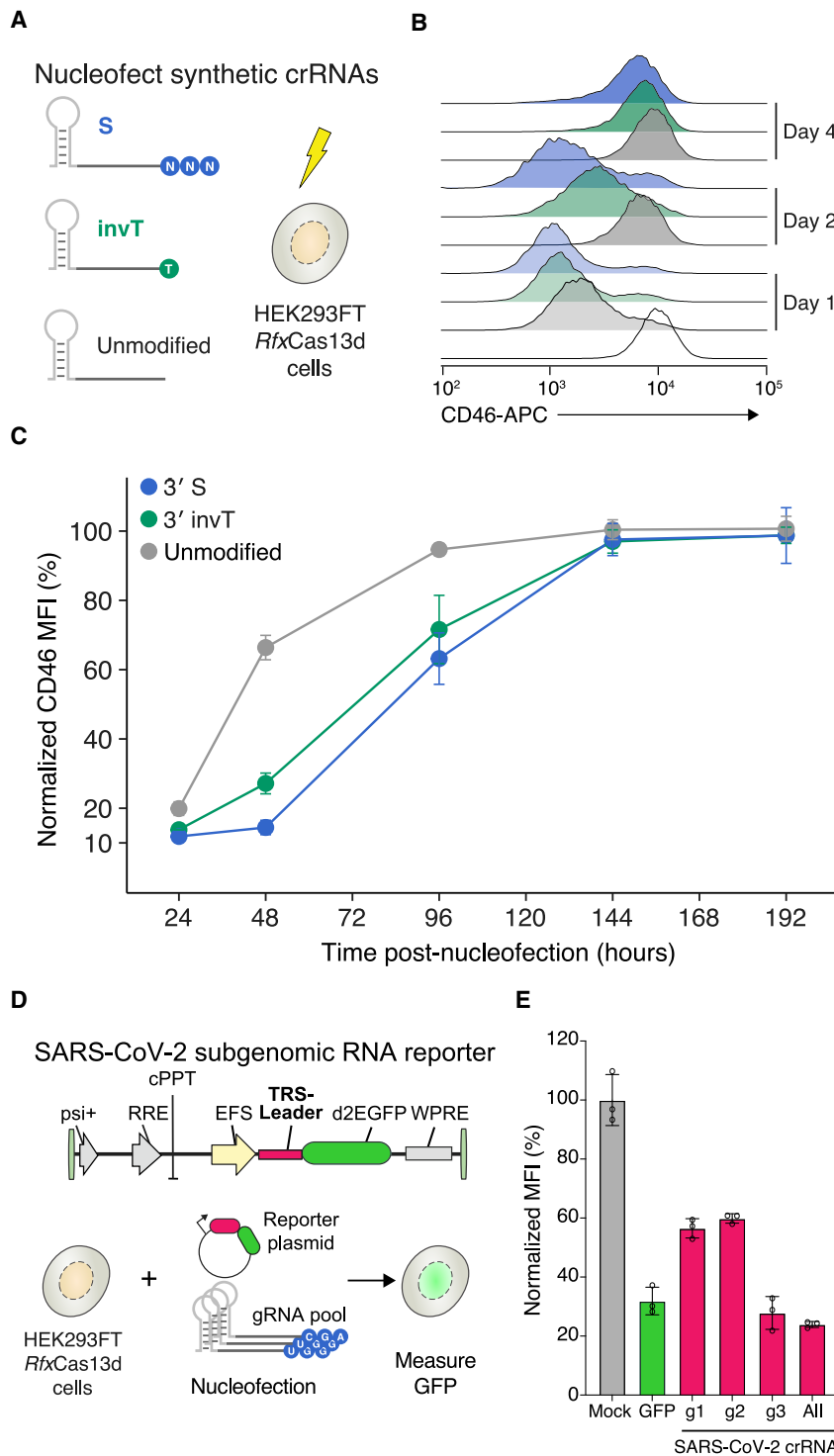


Figure 2. Transcript knockdown with chemically modified crRNAs is sustained over multiple days

(A) Experimental design to measure the temporal dynamics of transient CD46 knockdown by nucleofecting the synthetic crRNAs in the HEK293FT-TetO-RfxCas13d-NLS cells. Synthetic crRNAs were unmodified, chemically modified with a phosphorothioate bond (S) on three uridines at the 3' end, or chemically modified with an inverted thymidine at the 3' end (invT).

(B) Representative CD46 histograms at 1, 2, and 4 days after synthetic crRNA nucleofection.

(C) Relative CD46 protein expression upon nucleofection with the synthetic crRNAs in (A), normalized to cells nucleofected with non-targeting crRNAs. Points represent mean values \pm SD, n = 3 biological replicate nucleofections.

(D) Experimental approach to measure SARS-CoV-2 RNA knockdown using a subgenomic RNA fluorescent reporter (destabilized EGFP) with synthetic crRNAs chemically modified with a phosphorothioate bond (S) on the three terminal nucleotides of the guide sequence.

(E) EGFP expression in HEK293FT-TetO-RfxCas13d-NLS cells. Nucleofection conditions: GFP, pool of three S-modified crRNAs targeting EGFP; g1, g2, and g3, individual S-modified crRNAs targeting the SARS-CoV-2 TRS-Leader sequence; All, pool of g1, g2, and g3 S-modified crRNAs. Percentage GFP expression is determined relative to cells nucleofected with NT crRNAs. Bars represent mean values \pm SD, n = 3 biological replicate nucleofections.

essed CD46 expression in CD4+ and CD8+ populations separately 24 h after nucleofecting activated T cells (Figures 3E and S3E). For both T cell populations we achieved a 60%–65% knockdown of CD46 with 3'S-modified crRNAs (Figure 3F). With unmodified crRNAs, we achieved only 40%–45% knockdown of CD46. Taken together, these experiments demonstrate that Cas13 RNP can modify gene expression in primary immune cells and that modified crRNAs lead to greater gene knockdown than unmodified crRNAs.

DISCUSSION

Here, we show that chemically modified crRNAs can be used for Cas13d RNA targeting and knockdown. By testing different chemical modifications and their place-

ment within the crRNA, we identify a subset of optimal modifications for RNA targeting in cells and demonstrate that knockdown effects persist longer than with unmodified crRNAs. We show that crRNAs with 2'-O-methylation at bases on their 3' ends lead to improved knockdown of endogenous transcripts in human cells. We find similarly improved knockdown from phosphorothioate linkage but no added benefit to combining

chemically modified crRNAs also improves RNA knockdown with Cas13d RNPs (two-tailed paired t test, $p = 5 \times 10^{-3}$).

Using these optimized conditions for RNP formation and nucleofection, we isolated human T cells from healthy donors, stimulated the cells with anti-CD3 and anti-CD28 antibodies, and asked whether we could knockdown CD46 expression in primary T cells using these RNP complexes (Figure 3D). We as-

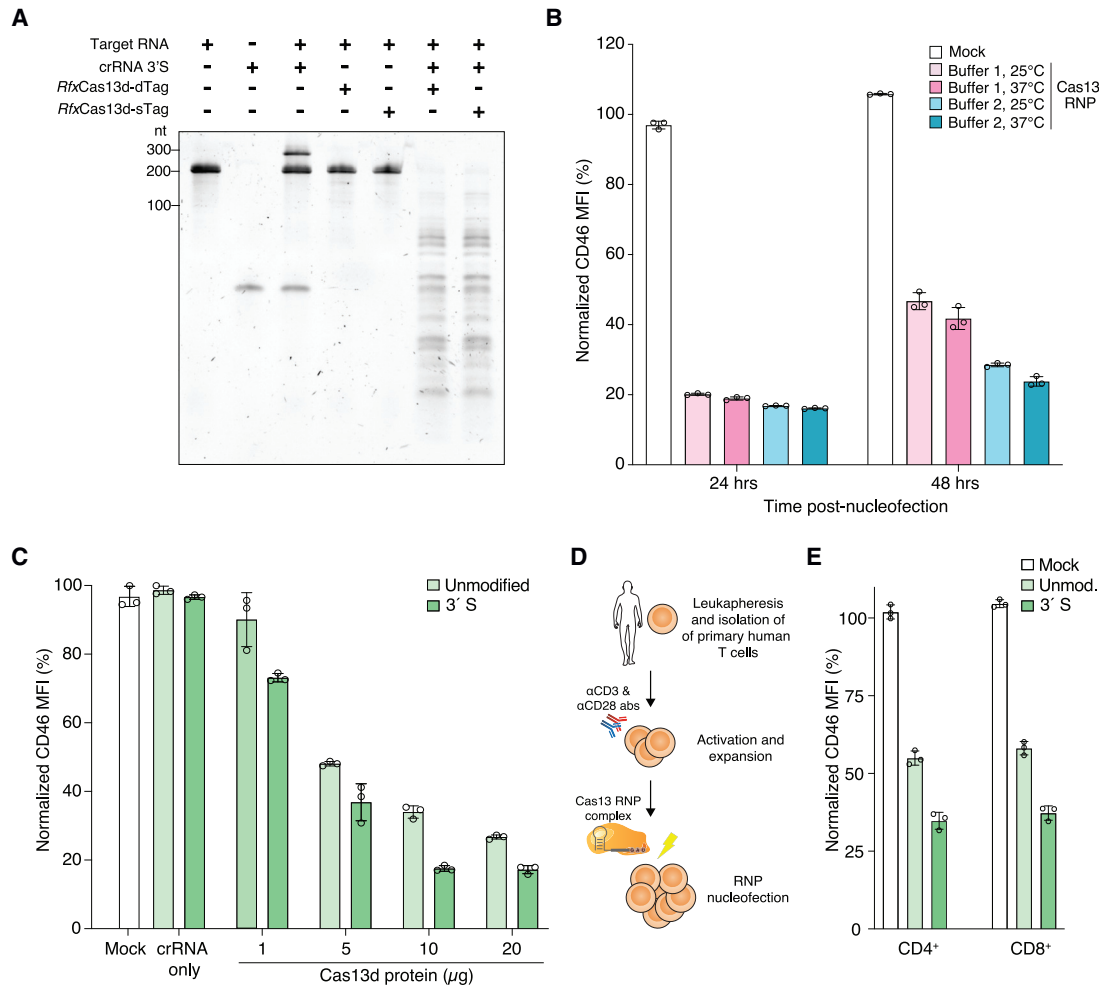


Figure 3. Robust knockdown in human cell lines and primary immune cells using Cas13d RNP complexes and chemically modified crRNAs
(A) Denaturing Tris-borate-EDTA (TBE)-urea gel showing the cleavage activity of the indicated *RfxCas13d* proteins tagged with either one (sTag) or two (dTag) affinity purification tags and their cleavage activity using a chemically modified crRNA (3'S) targeting CD46. *RfxCas13d-sTag* includes only a C-terminal hemagglutinin (HA) tag. *RfxCas13d-dTag* includes C-terminal HA and 6xHis tags and an N-terminal MKIEE solubility sequence.
(B) CD46 expression in HEK293FT cells at 24 and 48 h after nucleofection with Cas13 RNP complexed with buffer 1 (GenScript) and buffer 2 buffer (RNA cleavage buffer, see STAR Methods) at the indicated temperature prior to nucleofection.
(C) CD46 expression in HEK293FT cells at 24 h after nucleofection with synthetic crRNAs only and Cas13 RNP complexes with different protein amounts (1, 5, 10, and 20 μg) complexed with CD46-targeting synthetic crRNAs with no chemical modification or with a phosphorothioate bond at the 3' end (3'S).
(D) Leukapheresis and activation of primary human T cells prior to Cas13 RNP electroporation.
(E) CD46 expression in primary human T cells (CD4+ and CD8+) at 24 h after nucleofection with Cas13 RNPs complexed with CD46-targeting synthetic crRNAs with no chemical modification or with a 3'S modification. Bars represent mean values ±SD, n = 3 biological replicate nucleofections.

phosphorothioate linkages and 2'-O-methylation. It is also important where chemical modifications are placed in the crRNA: modification of the 3' end of the crRNA improves knockdown but more extensive modification is deleterious to Cas13 activity.

Furthermore, we demonstrate the use of Cas13d RNPs complexes together with chemically modified crRNAs in human cell lines and primary immune cells. Although chemically modified crRNAs improve knockdown with Cas13 from either an integrated transgene or from RNPs, the improvement is more modest for RNPs (~2-fold versus 4-fold), which suggests that the RNP complex may also protect the crRNA from degradation. Given the recent development of Cas13-based research tools,

diagnostics, and therapeutics (Konermann et al., 2018; Abbott et al., 2020; Fozzoni et al., 2020; Joung et al., 2020; Kushawah et al., 2020; Patchesung et al., 2020), chemically modified crRNAs can further enhance CRISPR-Cas13 RNA editing for diverse applications in biotechnology and medicine.

SIGNIFICANCE

The recent development of RNA-targeting CRISPR systems like Cas13 has enabled a wide variety of new methods for transcriptome engineering. Previously, we showed that optimization of the Cas13 crRNA sequence can boost nuclease activity on endogenous human transcripts. Here, we

systematically tested different crRNA chemical modifications, including 2'-O-methylation, phosphorothioate linkage, and an inverted thymidine cap, and their placement to identify key principles for optimized Cas13 targeting. We also developed effective Cas13 RNP complexes, providing a platform for non-viral delivery of Cas13. We demonstrated the utility of transcriptome engineering in several different applications, such as targeting endogenous human transcripts, antiviral defense against SARS-CoV-2 through the targeting the common leader sequence of viral subgenomic RNAs in a reporter construct, and in human primary cells, where CRISPR modifications have historically been challenging (in this case, primary CD8+ and CD4+ T cells). Our study highlights the utility of optimized, chemically modified crRNAs for efficient transcriptome engineering. We anticipate that chemically modified crRNAs for RNA-targeting CRISPRs will be useful for both *in vitro* RNA diagnostics and *in vivo* where DNA editing is not feasible or desirable.

STAR★METHODS

Detailed methods are provided in the online version of this paper and include the following:

- KEY RESOURCES TABLE
- RESOURCE AVAILABILITY
 - Lead contact
 - Materials availability
 - Data and code availability
- EXPERIMENTAL MODEL AND SUBJECT DETAILS
 - Cell line culture conditions
 - T cell isolation and culture conditions
- METHOD DETAILS
 - Plasmids
 - Chemically modified CRISPR RNA (crRNA) synthesis
 - Recombinant Cas13d production and purification
 - Nucleofection of crRNAs and ribonucleoprotein (RNP) complexes
 - Biochemical *in vitro* RNA cleavage assays
 - Flow cytometry
- QUANTIFICATION AND STATISTICAL ANALYSIS
 - Data analysis

SUPPLEMENTAL INFORMATION

Supplemental information can be found online at <https://doi.org/10.1016/j.chembiol.2021.07.011>.

ACKNOWLEDGMENTS

We thank the entire Sanjana laboratory for support and advice. N.E.S. is supported by NYU and NYGC startup funds, NIH/NHGRI (DP2HG010099), NIH/NCI (R01CA218668), NIH/NIGMS (R01GM138635), DARPA (D18AP00053), the Cancer Research Institute, and the Brain and Behavior Foundation. M.L. is a Hope Funds for Cancer Research fellow.

AUTHOR CONTRIBUTIONS

A.M.-M., H.H.W., and N.E.S. conceived the project. A.M.-M., H.H.W., and N.E.S. designed the experiments. A.M.-M. and H.H.W. performed *in vitro* and *in vivo* experiments. A.M.-M. and M.L. designed and performed experiments in primary T cells. A.K., J.W., and K.H. synthesized the crRNAs. M.M.

and G.B.R. produced recombinant Cas13d protein. A.M.-M., H.H.W., and N.E.S. wrote the manuscript with input from all of the authors.

DECLARATION OF INTERESTS

The New York Genome Center and New York University have applied for patents relating to the work in this article. M.M. and G.B.R. are employees of NEB. A.K., J.W., and K.H. are employees and shareholders of Synthego Corporation. N.E.S. is an adviser to Vertex and Qiagen.

Received: February 22, 2021

Revised: May 17, 2021

Accepted: July 8, 2021

Published: August 2, 2021

REFERENCES

- Abbott, T.R., Dhamdhare, G., Liu, Y., Lin, X., Goudy, L., Zeng, L., Chemparathy, A., Chmura, S., Heaton, N.S., Debs, R., et al. (2020). Development of CRISPR as an antiviral strategy to combat SARS-CoV-2 and influenza. *Cell* **181**, 865–876.
- Abudayyeh, O.O., Gootenberg, J.S., Essletzbichler, P., Han, S., Joung, J., Belanto, J.J., Verdine, V., Cox, D.B.T., Kellner, M.J., Regev, A., et al. (2017). RNA targeting with CRISPR-Cas13. *Nature* **550**, 280–284.
- Arizti-Sanz, J., Freije, C.A., Stanton, A.C., Boehm, C.K., Petros, B.A., Siddiqui, S., Shaw, B.M., Adams, G., Kosoko-Thoroddsen, T.S.F., Kember, M.E., et al. (2020). Integrated sample inactivation, amplification, and Cas13-based detection of SARS-CoV-2. *bioRxiv*. <https://doi.org/10.1101/2020.05.28.119131>.
- Barnes, K.G., Lachenauer, A.E., Nitido, A., Siddiqui, S., Gross, R., Beitzel, B., Siddle, K.J., Freije, C.A., Dighero-Kemp, B., Mehta, S.B., et al. (2020). Deployable CRISPR-Cas13a diagnostic tools to detect and report Ebola and Lassa virus cases in real-time. *Nat. Commun.* **11**, 4131.
- Basila, M., Kelley, M.L., and Smith, A.V.B. (2017). Minimal 2'-O-methyl phosphorothioate linkage modification pattern of synthetic guide RNAs for increased stability and efficient CRISPR-Cas9 gene editing avoiding cellular toxicity. *PLoS One* **12**, 1–19.
- Blanchard, E.L., Vanover, D., Bawage, S.S., Tiwari, P.M., Rotolo, L., Beyersdorf, J., Peck, H.E., Bruno, N.C., Hincapie, R., Michel, F., et al. (2021). Treatment of influenza and SARS-CoV-2 infections via mRNA-encoded Cas13a in rodents. *Nat. Biotechnol.* **39**, 717–726.
- Cox, D.B.T., Gootenberg, J.S., Abudayyeh, O.O., Franklin, B., Kellner, M.J., Joung, J., and Zhang, F. (2017). RNA editing with CRISPR-Cas13. *Science* **0180**, 1–15.
- Cromwell, C.R., Sung, K., Park, J., Krysler, A.R., Jovel, J., Kim, S.K., and Hubbard, B.P. (2018). Incorporation of bridged nucleic acids into CRISPR RNAs improves Cas9 endonuclease specificity. *Nat. Commun.* **9**, 1–11.
- Cui, J., Techakriengkrai, N., Nedumpun, T., and Suradhat, S. (2020). Abrogation of PRRSV infectivity by CRISPR-Cas13b-mediated viral RNA cleavage in mammalian cells. *Sci. Rep.* **10**, 9617.
- Fozouni, P., Son, S., Díaz de León Derby, M., Knott, G.J., Gray, C.N., D'Ambrosio, M.V., Zhao, C., Switz, N.A., Kumar, G.R., Stephens, S.I., et al. (2020). Amplification-free detection of SARS-CoV-2 with CRISPR-Cas13a and mobile phone microscopy. *Cell* **184**, 323–333.
- Freije, C.A., Myhrvold, C., Boehm, C.K., Lin, A.E., Welch, N.L., Carter, A., Metsky, H.C., Luo, C.Y., Abudayyeh, O.O., Gootenberg, J.S., et al. (2019). Programmable inhibition and detection of RNA viruses using Cas13. *Mol. Cell* **76**, 826–837.
- Gootenberg, J.S., Abudayyeh, O.O., Lee, J.W., Essletzbichler, P., Dy, A.J., Joung, J., Verdine, V., Donghia, N., Daringer, N.M., Freije, C.A., et al. (2017). Nucleic acid detection with CRISPR-Cas13a/C2c2. *Science* **356**, 438–442.
- Gootenberg, J.S., Abudayyeh, O.O., Kellner, M.J., Joung, J., Collins, J.J., and Zhang, F. (2018). Multiplexed and portable nucleic acid detection platform with Cas13, Cas12a and Csm6. *Science* **360**, 439–444.
- Granados-Riveron, J.T., and Aquino-Jarquín, G. (2018). CRISPR-Cas13 precision transcriptome engineering in cancer. *Cancer Res.* **4107–4114**.

- Guo, X., Wessels, H.-H., Méndez-Mancilla, A., Haro, D., and Sanjana, N.E. (2020). Transcriptome-wide Cas13 guide RNA design for model organisms and viral RNA pathogens. *bioRxiv*. <https://doi.org/10.1101/2020.08.20.259762>.
- Hendel, A., Bak, R.O., Clark, J.T., Kennedy, A.B., Ryan, D.E., Roy, S., Steinfeld, I., Lunstad, B.D., Kaiser, R.J., Wilkens, A.B., et al. (2015). Chemically modified guide RNAs enhance CRISPR-Cas genome editing in human primary cells. *Nat. Biotechnol.* **33**, 985–989.
- Jiang, T., Henderson, J.M., Coote, K., Cheng, Y., Valley, H.C., Zhang, X.O., Wang, Q., Rhym, L.H., Cao, Y., Newby, G.A., et al. (2020). Chemical modifications of adenine base editor mRNA and guide RNA expand its application scope. *Nat. Commun.* **11**, 1–9.
- Joung, J., Ladha, A., Saito, M., Kim, N.G., Woolley, A.E., Segel, M., Barretto, R.P.J., Ranu, A., Macrae, R.K., Faure, G., et al. (2020). Detection of SARS-CoV-2 with SHERLOCK one-pot testing. *N. Engl. J. Med.* **383**, 2018–2021.
- Kim, D., Lee, J.Y., Yang, J.S., Kim, J.W., Kim, V.N., and Chang, H. (2020). The architecture of SARS-CoV-2 transcriptome. *Cell* **181**, 914–921.
- Konermann, S., Lotfy, P., Brideau, N.J., Oki, J., Shokhirev, M.N., and Hsu, P.D. (2018). Transcriptome engineering with RNA-targeting type VI-D CRISPR effectors. *Cell* **173**, 665–676.
- Kushawah, G., Hernandez-Huertas, L., Abugattas-Núñez del Prado, J., Martínez-Morales, J.R., DeVore, M.L., Hassan, H., Moreno-Sanchez, I., Tomas-Gallardo, L., Díaz-Moscoso, A., Monges, D.E., et al. (2020). CRISPR-Cas13d induces efficient mRNA knockdown in animal embryos. *Dev. Cell* **54**, 805–817.
- Lai, M.M.C. (1986). Coronavirus leader-RNA-primed transcription: an alternative mechanism to RNA splicing. *BioEssays* **5**, 257–260.
- Lee, K., Mackley, V.A., Rao, A., Chong, A.T., Dewitt, M.A., Corn, J.E., and Murthy, N. (2017). Synthetically modified guide RNA and donor DNA are a versatile platform for CRISPR-Cas9 engineering. *eLife* **6**, 1–17.
- Li, J., Chen, Z., Chen, F., Xie, G., Ling, Y., Peng, Y., Lin, Y., Luo, N., Chiang, C.M., and Wang, H. (2020). Targeted mRNA demethylation using an engineered dCas13b-ALKBH5 fusion protein. *Nucleic Acids Res.* **48**, 5684–5694.
- McMahon, M.A., Prakash, T.P., Cleveland, D.W., Bennett, C.F., and Rahdar, M. (2018). Chemically modified cpf1-CRISPR RNAs mediate efficient genome editing in mammalian cells. *Mol. Ther.* **26**, 1228–1240.
- Patchesung, M., Jantarug, K., Pattama, A., Aphicho, K., Suraritdechchai, S., Meesawat, P., Sappakhaw, K., Leelahakorn, N., Ruenkam, T., Wongsatit, T., et al. (2020). Clinical validation of a Cas13-based assay for the detection of SARS-CoV-2 RNA. *Nat. Biomed. Eng.* **4**, 1140–1149.
- Ribas, A., and Wolchok, J.D. (2018). Cancer immunotherapy using checkpoint blockade. *Science* **359**, 1350–1355.
- Ryan, D.E., Taussig, D., Steinfeld, I., Phadnis, S.M., Lunstad, B.D., Singh, M., Vuong, X., Okochi, K.D., McCaffrey, R., Olesiak, M., et al. (2018). Improving CRISPR-Cas specificity with chemical modifications in single-guide RNAs. *Nucleic Acids Res.* **46**, 792–803.
- Smargon, A.A., Shi, Y.J., and Yeo, G.W. (2020). Metagenomic discovery to transcriptomic engineering. *Nat. Cell Biol.* **22**, 143–150.
- Smith, T.T., Stephan, S.B., Moffett, H.F., McKnight, L.E., Ji, W., Reiman, D., Bonagofski, E., Wohlfahrt, M.E., Pillai, S.P.S., and Stephan, M.T. (2017). In situ programming of leukaemia-specific t cells using synthetic DNA nanocarriers. *Nat. Nanotechnol.* **12**, 813–822.
- Wang, H., Nakamura, M., Abbott, T.R., Zhao, D., Luo, K., Yu, C., Nguyen, C.M., Lo, A., Daley, T.P., Russa, M.L., et al. (2019). CRISPR-mediated live imaging of genome editing and transcription. *Science* **365**, 1301–1305.
- Wang, S.R., Wu, L.Y., Huang, H.Y., Xiong, W., Liu, J., Wei, L., Yin, P., Tian, T., and Zhou, X. (2020). Conditional control of RNA-guided nucleic acid cleavage and gene editing. *Nat. Commun.* **11**, 91.
- Wessels, H.H., Méndez-Mancilla, A., Guo, X., Legut, M., Danilowski, Z., and Sanjana, N.E. (2020). Massively parallel Cas13 screens reveal principles for guide RNA design. *Nat. Biotechnol.* **38**, 722–727.
- Wienert, B., Shin, J., Zelin, E., Pestal, K., and Corn, J.E. (2018). In vitro-transcribed guide RNAs trigger an innate immune response via the RIG-I pathway. *PLoS Biol.* **16**, 1–18.
- Yang, L.Z., Wang, Y., Li, S.Q., Yao, R.W., Luan, P.F., Wu, H., Carmichael, G.G., and Chen, L.L. (2019). Dynamic imaging of RNA in living cells by CRISPR-cas13 systems. *Mol. Cell* **76**, 981–997.
- Yin, H., Song, C.Q., Suresh, S., Wu, Q., Walsh, S., Rhym, L.H., Mintzer, E., Bolukbasi, M.F., Zhu, L.J., Kauffman, K., et al. (2017). Structure-guided chemical modification of guide RNA enables potent non-viral in vivo genome editing. *Nat. Biotechnol.* **35**, 1179–1187.
- Zhang, C., Konermann, S., Brideau, N.J., Lotfy, P., Wu, X., Novick, S.J., Strutzenberg, T., Griffin, P.R., Hsu, P.D., and Lyumkis, D. (2018). Structural basis for the RNA-guided ribonuclease activity of CRISPR-cas13d. *Cell* **175**, 212–223.

STAR★METHODS

KEY RESOURCES TABLE

REAGENT or RESOURCE	SOURCE	IDENTIFIER
Antibodies		
CD46 clone TRA-2-10	Biolegend	Cat# 352405; RRID: AB_2564356
CD55 clone JS11	Biolegend	Cat# 311305; RRID: AB_314862
CD71 (TFRC) clone CYIG4	Biolegend	Cat# 334105; RRID: AB_2271603
Bacterial and virus strains		
NEB Stable Cells	New England Biolabs	Cat #C3040I
<i>E. coli</i> NiCo21(DE3)	New England Biolabs	Cat #C2529
Biological samples		
Buffy coats (leukocytes)	New York Blood Center	https://nybloodcenter.org/
Chemicals, peptides, and recombinant proteins		
Lymphoprep	Stem Cell technologies	Cat #07811
Recombinant human IL-2	Stem Cell Technologies	Cat #78081
ImmunoCult Human CD3/CD28 T cell Activator	Stem Cell Technologies	Cat #10991
Kanamycin	Sigma-Aldrich	Cat #K1377
IPTG	Sigma-Aldrich	Cat #I6758
Doxycycline hydrochloride	Sigma-Aldrich	Cat #D3447
LIVE/DEAD Fixable Violet Dead Cell Stain	ThermoFisher Scientific	Cat #L34963
Nuclease Buffer 10X	GenScript	Cat #SC1841
2X RNA Gel Loading Dye	Thermo Fisher Scientific	Cat #R0641
Novex 10% TBE-Urea gels	Thermo Fisher Scientific	Cat #EC68752BOX
Critical commercial assays		
EasySep Human CD8 Positive Selection Kit	Stem Cell technologies	Cat #17853
EasySep Human CD4 T cell Isolation Kit	Stem Cell technologies	Cat #17952
Bradford assay	Bio-Rad	Cat #5000201
Direct-zol RNA MicroPrep	Zymo Research	Cat #R2061
SF Cell Line Nucleofector Solution	Lonza	Cat #V4XC-2032
P3 Primary Cell Nucleofector Solution	Lonza	Cat #V4XP-3032
RevertAid RT Reverse Transcription Kit	Thermo Fisher Scientific	Cat #K1691
HiScribe T7 High Yield RNA Synthesis Kit	New England Biolabs	Cat #E2040S
HiScribe T7 ARCA mRNA Kit	New England Biolabs	Cat #E2060S
Monarch RNA Cleanup Kit	New England Biolabs	Cat #T2050S
Experimental models: cell lines		
HEK293FT	Thermo Fisher Scientific	Cat#R70007
HEK293FT-RfxCas13d-NLS	This paper	NA
Experimental models: organisms/strains		
Oligonucleotides		
Please refer to Tables S2 and S3		
Recombinant DNA		
pLenti-TRS-Leader-SARS-CoV-2-EGFP	This paper	Addgene 171585
pET28-His-MBP-NLS-RfxCas13d-NLS-HA	This paper	Addgene 171586
pET28-MKIEE-NLS-RfxCas13d-NLS-HA-6His	This paper	Addgene 171587
pLentiRNACRISPR_007 - TetO-NLS-RfxCas13d-NLS-WPRE-EFS-rtTA3-2A-Blast	Wessels et al., 2020	Addgene 138149

(Continued on next page)

Continued

REAGENT or RESOURCE	SOURCE	IDENTIFIER
pMD2.G	Trono Lab packaging and envelope plasmids	Addgene 12259
psPAX2	Trono Lab packaging and envelope plasmids	Addgene 12260

Software and algorithms

GraphPad Prism 8	GraphPad	https://www.graphpad.com/
FlowJo 10	Becton, Dickinson and Company	https://www.flowjo.com/solutions/flowjo
Cas13 design tool	Guo et al. (2020)	https://cas13design.nygenome.org/

Other

HiTrapDEAEFF Sepharose columns	Cytiva	Cat #17505401
HisTrap HP columns	Cytiva	Cat #17524701
HiTrap HeparinHP columns	Cytiva	Cat #17040703

RESOURCE AVAILABILITY

Lead contact

Further information requests should be directed to the lead contact, Neville Sanjana (neville@sanjanalab.org).

Materials availability

Plasmids (TRS-Leader-SARS-CoV-2-d2eGFP, pET28-His-MBP-NLS-RfxCas13d-NLS-HA and pET28-MKIEE-NLS-RfxCas13d-NLS-HA-6His) have been deposited with Addgene (plasmid nos. 171585, 171586, 171587).

Data and code availability

Data will be shared by the lead contact upon request. This paper does not report original code. Cas13 guide RNAs were designed using *cas13design* (<https://cas13design.nygenome.org/>). Additional information required to reanalyze the data reported in this paper is available from the lead contact upon request.

EXPERIMENTAL MODEL AND SUBJECT DETAILS

Cell line culture conditions

HEK293FT cells were acquired from Thermo Fisher Scientific (R70007) and maintained in D10 media: DMEM with high glucose and stabilized L-glutamine (Caisson DML23) supplemented with 10% Serum Plus II fetal bovine serum (Sigma-Aldrich 14009C) and no antibiotics. For Tet-free D10 media, we omitted the Serum Plus II and instead substituted 10% tetracycline-negative fetal bovine serum (Corning 35-075-CV) for the Serum Plus II. HEK293FT were cultured at 37°C, 5% CO₂, and ambient oxygen levels. We generated doxycycline-inducible HEK293FT-RfxCas13d-NLS cells using lentiviral transduction (Wessels et al., 2020).

T cell isolation and culture conditions

T cells were procured from a de-identified healthy donor LeukoPak (New York Blood Center). Peripheral blood mononuclear cells (PBMCs) were isolated using Lymphoprep density gradient centrifugation (StemCell Technologies). CD8⁺ T cells were isolated from PBMCs by positive magnetic selection using EasySep Human CD8 Positive Selection Kit (StemCell Technologies). CD4⁺ T cells were isolated from PBMCs by negative magnetic selection using EasySep Human CD4 T cell Isolation Kit (StemCell Technologies). Isolated T cells were then plated in ImmunoCult-XF T Cell Expansion Medium (StemCell Technologies) supplemented with 10 ng μL⁻¹ recombinant human IL-2 (StemCell Technologies) and activated with the ImmunoCult Human CD3/CD28 T Cell Activator (StemCell Technologies). T cells were cultured at 37°C, 5% CO₂, and ambient oxygen levels.

METHOD DETAILS

Plasmids

We cloned the TRS-Leader-SARS-CoV-2-d2eGFP plasmid (Addgene 171585) by introducing 75 nt of the SARS-CoV-2 Leader sequence into the *NheI*-digested EFS-EGFPd2PEST-2A-Hygro plasmid (Addgene 138152). We inserted the TRS-Leader immediately before the coding sequence by ligation of annealed oligos (see Table S3 for sequences). We generated bacterial RfxCas13d expression vectors as follows. Codon-optimized cDNAs containing the effector protein RfxCas13d were synthesized (Genscript) and assembled into modified pET28 vectors by NEBuilder HiFi DNA assembly (E2621, NEB). We created 2 bacterial expression

vectors: pET28-His-MBP-NLS-RfxCas13d-NLS-HA (Addgene 171586) produces the protein *RfxCas13d*-sTag after cleavage of the N-terminal His-MBP fusion partner, and pET28-MKIEE-NLS-RfxCas13d-NLS-HA-6His (Addgene 171587) produces the protein *RfxCas13d*-dTag. For both constructs, NLS indicates the nuclear localization sequence derived from the simian virus 40 (SV40) large T-antigen.

Chemically modified CRISPR RNA (crRNA) synthesis

The crRNAs were synthesized using solid-phase phosphoramidite chemistry (Synthego CRISPRRevolution platform). Following synthesis, postprocessing and purification steps, we quantified each crRNA by UV absorption using Nanodrop (Thermo). We confirmed their identities and quality using an Agilent 1290 Infinity II high-performance liquid chromatography (HPLC) system coupled with an Agilent 6530B Quadrupole time of-flight mass spectrometry (Agilent Technologies) in negative ion polarity mode.

Recombinant Cas13d production and purification

Recombinant *RfxCas13d* proteins were expressed in *E. coli* NiCo21(DE3) (NEB C2529). Cells were grown in 1L of lysogeny (Luria-Bertani) broth containing 40 mg/mL kanamycin with shaking at 30°C. Protein expression was induced by the addition of 0.4 mM IPTG and the temperature was reduced to 16°C for 16 hours. Pelleted cells were disrupted by sonication. Proteins were purified from the lysate supernatant using HiTrapDEAE^{FF} Sepharose, HiTrap HP and HiTrap HeparinHP columns on an Akta Go instrument (Cytiva). To produce sTag *RfxCas13d*, the N-terminal His-MBP fusion partner was cleaved with Sumo protease and removed. Purified *RfxCas13d* proteins were stored in 20mM Tris-HCl, pH7.5, 500mM NaCl, 1mM EDTA, 1mM DTT and 50% glycerol (v/v). Protein concentration was determined by Bradford assay (Bio-Rad).

Nucleofection of crRNAs and ribonucleoprotein (RNP) complexes

For nucleofection experiments in HEK293FT-*RfxCas13d* cells, we seeded three replicates of $\sim 2 \times 10^6$ cells in D10 media with 1 μ g/mL of doxycycline 24 hours before nucleofection. Using 1×10^5 cells per condition/nucleofection, we nucleofected HEK293FT-*RfxCas13d* cells with 225 μ mol of synthetic crRNAs in 20 μ l reaction of SF Cell Line Nucleofector Solution (Lonza V4XC-2032) using the Lonza Nucleofector 4D (program CM-130). Immediately after nucleofection, we plated cells in pre-equilibrated D10 media (equilibrated to 37°C and 5% CO₂). For SARS-CoV-2 RNA knockdown, we nucleofected HEK293FT-*RfxCas13d* with 0.4 μ g of TRS-Leader-SARS-CoV-2-d2eGFP plasmid together with 225 μ mol of synthetic crRNAs and performed flow cytometry 24 hours after nucleofection.

For RNP delivery experiments, purified *RfxCas13d* protein and crRNAs were assembled at a 1:2 molar ratio (Cas13 protein : crRNA) under two different RNP complexing conditions: 1) 10 mins at 25°C or 37°C with nuclease reaction buffer (GenScript) and 2) 15 mins at 24°C or 37°C with RNA cleavage buffer (25mM Tris pH 7.5, 1mM DTT, 6mM MgCl₂). After complexing, the *RfxCas13d* RNPs were nucleofected into HEK293FT cells or primary T cells using 10^5 to 10^6 cells in 20 μ l of nucleofection solutions specific for each cell type. For HEK293FT nucleofection, cells were nucleofected in 20 μ l reaction of SF Cell Line Nucleofector Solution (Lonza V4XC-2032) using the Lonza Nucleofector 4D (program CM-130). Immediately after nucleofection, HEK293FT cells were plated in pre-equilibrated D10 media (equilibrated to 37°C and 5% CO₂) and remained there until flow cytometry analysis. For T cells nucleofection, two days after activation CD4+ and CD8+ T cells were combined, washed 2X in Dulbecco's PBS without calcium or magnesium (D-PBS, Caisson Labs) and resuspended in 20 μ l P3 Primary Cell Nucleofector Solution (Lonza V4XP-3032). T cells were then nucleofected using the Lonza Nucleofector 4D (program E0-115). Nucleofections were performed in triplicate. Immediately after nucleofection T cells were plated in pre-equilibrated ImmunoCult-XF T Cell Expansion Medium supplemented with 10 ng μ L⁻¹ recombinant human IL-2 (equilibrated to 37°C and 5% CO₂). Before flow cytometry analysis, nucleofected T cells were washed with D-PBS and stained with LIVE/DEAD Fixable Violet Dead Cell Stain (ThermoFisher) for 5 minutes at room temperature in the dark before proceeding with antibody stain.

Biochemical *in vitro* RNA cleavage assays

We synthesized 200 bp target RNAs for CD46, CD55 and CD71 by PCR amplification of templates from total cDNA from HEK293FT cells and then performed T7 *in vitro* RNA transcription. To prepare the cDNA library, we extracted total RNA from HEK293FT cells using Direct-zol purification (Zymo) and reverse transcribed 1 μ g of RNA into cDNA using Revert-Aid (ThermoFisher). Using the PCR templates of target RNAs, we performed *in vitro* RNA transcription using the HiScribe T7 High Yield RNA Synthesis Kit (NEB). After transcription, RNA was purified using a Monarch RNA Cleanup Kit (NEB) and quantified on a Nanodrop spectrophotometer (Thermo).

Similarly, *RfxCas13d* and eGFP messenger RNAs (mRNAs) were synthesized using a T7 RNA polymerase *in vitro* transcription with the HiScribe T7 ARCA mRNA Kit (with tailing) (NEB). The mRNAs were purified using a Monarch RNA Cleanup Kit (NEB). We amplified target RNAs and mRNAs using primers that include a T7 promoter sequence on the 5' end; for the mRNAs, we also included the corresponding Kozak and start/stop codon sequences (Table S2).

Purified *RfxCas13d* proteins and synthetic crRNAs were mixed (unless otherwise indicated) at a 1:2 molar ratio in Buffer 1 (GenScript SC1841) or Buffer 2 (Konermann et al., 2018) (25mM Tris pH 7.5, 1mM DTT, 6mM MgCl₂). The reaction was prepared on ice and incubated at 25°C or 37°C for 15 minutes prior to the addition of target RNA at 1:2 molar ratio relative to *RfxCas13d* protein. The reaction was incubated at 37°C for 45 minutes and quenched with 1 μ L of enzyme stop solution (Konermann et al., 2018) (10 mg/mL Proteinase K, 4M Urea, 80mM EDTA, 20mM Tris pH 8.0) at 37°C for 15 minutes. The samples were denatured at 95°C for 5 minutes

in 2X RNA Gel Loading Dye (ThermoFisher) and loaded onto Novex 10% TBE-Urea gels (ThermoFisher). The gels were run at 180 V for 35 mins. After separation, gels were stained with SYBR Gold (ThermoFisher) prior to imaging via Gel Doc EZ system (Bio-Rad).

Flow cytometry

Cells were stained with the following antibodies: PE anti-human CD4 (clone RPA-T4, Biolegend 300507), FITC anti-human CD8a (clone RPA-T8, Biolegend 301006) and APC anti-human CD46 (clone TRA-2-10, Biolegend 352405). Antibody staining was performed for 20 minutes on ice. After staining the cells were washed 2X in D-PBS and analyzed via flow cytometry (Sony SH800S). A minimum of 10,000 viable events was collected per sample.

QUANTIFICATION AND STATISTICAL ANALYSIS

Data analysis

Data analysis and statistical testing was performed using GraphPad Prism 8 (GraphPad Software Inc.). Flow cytometry analysis and figure generation was performed using FlowJo v10 (BD). Specific statistical analysis methods are described where results are presented.